Critical Reviews in Biochemistry and Molecular Biology, 2010; 45(3): 243–256

informa
healthcare

REVIEW ARTICLE

Insights into the MCM functional mechanism: lessons learned from the archaeal MCM complex

Aaron S. Brewster, and Xiaojiang S. Chen

Molecular and Computational Biology, University of Southern California, Los Angeles, CA 90089, USA

Abstract
The helicase function of the minichromosome maintenance protein (MCM) is essential for genomic DNA replication in archaea and eukaryotes. There has been rapid progress in studies of the structure and function of MCM proteins from different organisms, leading to better understanding of the MCM helicase mechanism. Because there are a number of excellent reviews on this topic, we will use this review to summarize some of the recent progress, with particular focus on the structural aspects of MCM and their implications for helicase function. Given the hexameric and double hexameric architecture observed by X-ray crystallography and electron microscopy of MCMs from archaeal and eukaryotic cells, we summarize and discuss possible unwinding modes by either a hexameric or a double hexameric helicase. Additionally, our recent crystal structure of a full length archaeal MCM has provided structural information on an intact, multi-domain MCM protein, which includes the salient features of four unusual β-hairpins from each monomer, and the side channels of a hexamer/double hexamer. These new structural data enable a closer examination of the structural basis of the unwinding mechanisms by MCM.

Keywords: *DNA replication; replicative helicase; nucleic-acid motor; β-hairpin; AAA+ initiator protein*

Introduction

Minichromosome maintenance protein (MCM) is a DNA helicase essential for genomic DNA replication (Forsburg, 2004; Moyer *et al.*, 2006; Bochman and Schwacha, 2008). As a critical protein for cell division, MCM is also the target of various checkpoint pathways, such as the S-phase entry and S-phase arrest checkpoints (Forsburg, 2008). Both the loading and activation of MCM helicase are strictly regulated and are coupled to cell growth cycles. De-regulation of MCM function has been linked to genomic instability and a variety of carcinomas (Forsburg, 2004, Lau *et al.*, 2007).

Eukaryotic MCM consists of six gene products, MCM2–7, which form a heterohexamer (Bell and Dutta, 2002). While for years *in vitro* helicase activity could not be observed, recent reports have identified such activity for the heterohexamer (Moyer *et al.*, 2006; Bochman and Schwacha, 2008). A great deal of biochemical data has been collected regarding the heterohexamer, as well as the dimer of the trimer MCM 4, 6, 7, which also exhibits helicase activity (Ishimi, 1997; You *et al.*, 1999; Lee and Hurwitz, 2001). However, high resolution structural studies with heterohexameric eukaryotic proteins are lagging behind.

Archaeal replication systems share many similarities to eukaryotic systems, including archaeal MCM proteins that are homologous to the eukaryotic MCM proteins (Kelman and White, 2005). Most archaeal genomes sequenced so far have revealed the presence of only one MCM gene, which makes archaeal MCM a simpler system for understanding the MCM structure and function relationship. So far, perhaps the best studied MCM proteins are from the species *M. thermoautotrophicum* (mthMCM) and *S. solfataricus* (ssoMCM). Both proteins oligomerize to form double-hexamers or hexamers in solution (Kelman *et al.*, 1999; Chong *et al.*, 2000; Carpentieri *et al.*, 2002; Fletcher *et al.*, 2003). Both exhibit single- and double-stranded DNA binding, a basal ATPase activity stimulated by the addition of DNA, and 3′→5′ helicase activity on forked

Address for Correspondence: Xiaojiang S. Chen, 1050 Child's Way, Los Angeles, CA 90089, USA. Tel: 213 740 5487. Email: xiaojiac@usc.edu

(Received 09 December 2009; revised 30 March 2010; accepted 08 April 2010)

ISSN 1040-9238 print/ISSN 1549-7798 online © 2010 Informa UK Ltd
DOI: 10.3109/10409238.2010.484836

DNA substrate *in vitro* (Kelman *et al.*, 1999; Chong *et al.*, 2000; Carpentieri *et al.*, 2002; Fletcher *et al.*, 2003; Pucci *et al.*, 2004).

In contrast to the lagging eukaryotic structural studies, recently there has been great progress in the structural studies of archaeal MCM proteins, which has provided valuable information for understanding the MCM helicase mechanism. Currently, the following X-ray structures have been determined: the N-terminal structures for mthMCM (Fletcher *et al.*, 2003) and ssoMCM (Liu *et al.*, 2008), a near full-length ssoMCM structure (Figure 1) (Brewster *et al.*, 2008), and an MCM homolog from another archaeon, *M. kandleri* (mkaMCM2) (Bae *et al.*, 2009) (reviewed in Sakakibara *et al.*, 2009).

The two recent structures have issues that affect analysis. The near full-length ssoMCM was solved to a low resolution (4.35 Å) and is therefore a poly-alanine structure. The registry of the amino-acid sequence was verified through identification of heavy atom selenomethionine peaks in the electron density maps, but caution should still be exercised. Also, while mkaMCM2 was solved to higher resolution (1.9 Å), it has a natural deletion of a critical zinc-binding sub-domain in the N-terminal domain, which prevents hexamerization and thus helicase activity. MkaMCM2 also lacks canonical ATP-binding residues, resulting in no ATPase activity (Bae *et al.*, 2009). Finally, while full-length ssoMCM crystals were available, in the final structure the most C-terminal 85 residues (residues 602–686, predicted to form a winged helix fold), are missing, likely due to the flexibility of this domain. This domain is also naturally deleted in mkaMCM2. We will mainly focus on the interpretation of the near full-length ssoMCM structure in the following discussion, but most of the structural features of mkaMCM2 bear out the conclusions.

Regardless of the above issues, the new structures allow us to predict models relating to the structure–function relationship of MCM. In this article we first briefly review MCM structure, then examine how current biochemical data combines with the structures to present models for DNA unwinding, both in regards to where in the enzyme DNA is bound, and how ATP binding and hydrolysis may trigger conformational changes (domain and hairpin movement) to catalyze strand separation.

Overview of MCM structure

The ssoMCM structure reveals an elongated fold, with two large N- and C-terminal domains (Figure 1). The N-terminal domain (or N-domain, residues 1–266) consists of three small sub-domains and appears to be used mainly for structural organization (Fletcher *et al.*, 2003, Liu *et al.*, 2008), and possibly for processivity (Barry *et al.*, 2007). The N-domain can coordinate with a neighboring subunit's C-terminal AAA+ (ATPases Associated with diverse cellular Activities) helicase domain (residues 276–601) through a long and conserved loop (Brewster *et al.*, 2008). This conserved loop, named the allosteric control loop (ACL), has been shown to play a role in regulating interactions between N- and C-terminal regions by facilitating communication between the domains in response to ATP hydrolysis (Brewster *et al.*, 2008; Sakakibara *et al.*, 2008; Barry *et al.*, 2009). Further, the N-domain establishes the *in vitro* 3′→5′ directionality of ssoMCM when added in trans- to the separated C-terminal domain *in vitro* (Barry *et al.*, 2007).

The sequence of the C-terminal domain (or C-domain, residues 276–686) is well conserved across species and between MCM subfamilies (Tye and Sawyer, 2000). The C-domain consists of an AAA+ ATPase core and a small winged helix bundle, and is the site of ATP hydrolysis and DNA unwinding. ATP binding and hydrolysis occurs at an interface between two monomers; one monomer provides the tri-phosphate binding loop (p-loop or Walker A/B motifs) for ATP binding in cis- and the other

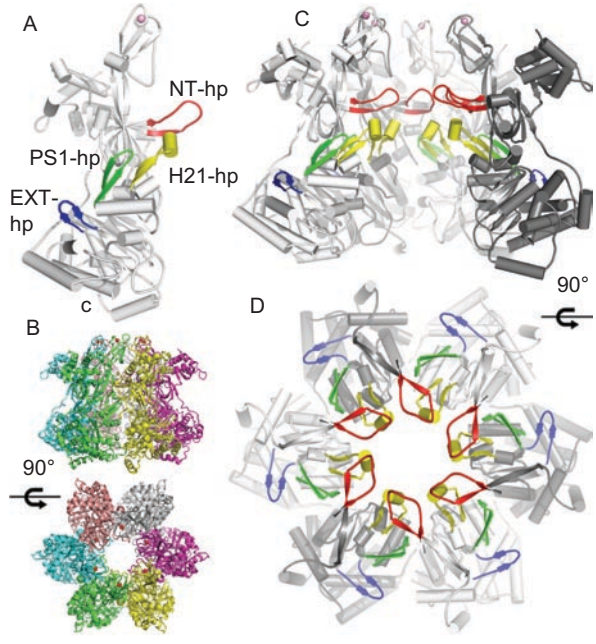

Figure 1. The salient features of the four β-hairpins of ssoMCM. (A) SsoMCM monomer (Brewster *et al.*, 2008). N- and C-terminal ends are labeled. Pink sphere: zinc atom. The four β-hairpins are colored and labeled. NT-hp (red): N-domain hairpin. H2I-hp (yellow): helix-2 insert. PS1-hp (green): pre-sensor 1 hairpin. EXT-hp (blue): exterior hairpin. (B) Two different views of the ssoMCM hexamer structural model. Individual subunits are colored differently. (C) Side view of ssoMCM hexamer colored as in A, with two monomers in the front removed to reveal the β-hairpins in the central and side channels. (D) Top view of ssoMCM hexamer, showing the β-hairpins in the central and side channels. Most of the N-domain, except the NT-hp, has been removed for clarity.

monomer contributes residues in trans- to interact with the ATP (Iyer *et al.*, 2004; Brewster *et al.*, 2008).

MkaMCM2 was crystallized as a monomer, as was the full length ssoMCM, despite the fact that ssoMCM forms a hexamer in solution and shows helicase activity (Brewster *et al.*, 2008; Bae *et al.*, 2009). However, the mthMCM N-domain (N-mthMCM) was crystallized as a double hexamer, with two hexamers stacked in a "head to head" configuration (Fletcher *et al.*, 2003), and the ssoMCM N-domain (N-ssoMCM) was crystallized as a single hexamer (Liu *et al.*, 2008). Not so surprisingly, the structures of the N-mthMCM and the N-ssoMCM hexamers are very similar to each other, and can be aligned quite well. Thus, these hexamers of the N-domains of MCMs can be used to model the hexamer conformation of the full-length ssoMCM protein (Figure 1B).

Based on the N-mthMCM hexameric structure, a hexamer model for the near-full-length ssoMCM structure was generated (Brewster *et al.*, 2008). The near-full-length (FL) hexameric model exhibits a dumbbell appearance from the side, with a slim or narrow "waist" between the N- and C-domains. This general shape has been confirmed by electron microscopy (EM) studies (Pape *et al.*, 2003; Gómez-Llorente *et al.*, 2005; Costa *et al.*, 2006a). The central channel of the modeled hexamer has dimensions that can accommodate ssDNA or dsDNA (Fletcher *et al.*, 2003; Brewster *et al.*, 2008). Further, six side channels extend radially through the side "wall" of the C-terminal helicase domain near the N-terminal side of the ATP binding pocket. These side channels are visible by EM in archaea (Pape *et al.*, 2003; Gómez-Llorente *et al.*, 2005; Costa *et al.*, 2006a) and eukaryotes (Remus *et al.*, 2009) and appear wide enough to allow ssDNA to be threaded through, as was proposed for the side channels seen in the SV40 Large T antigen (LTag) hexameric helicase structures (Li *et al.*, 2003; Gai *et al.*, 2004b). Another salient feature is that each monomer has four types of β-hairpin structures that are located around the central and side channels: one in the N-domain called the NT-hairpin (or NT-hp), and three in the C-domain, named exterior hairpin (EXT-hp), helix 2 insert hairpin (H2I-hp), and pre-sensor 1 hairpin (PS1-hp) (see Figures 1A, 1C, 1D, 2A and 2B).

The NT-hp projects into the central channel where it binds DNA (Fletcher *et al.*, 2003; McGeoch *et al.*, 2005). Mutations involving important basic residues on the tip of this hairpin weaken ssDNA and dsDNA binding, and proportionally affect helicase activity in line with the lessening of DNA binding (McGeoch *et al.*, 2005). The PS1-hp located N-terminal to the sensor-1 asparagine in the C-terminal AAA+ domain also has a critical lysine on its tip which affects DNA binding (McGeoch *et al.*, 2005). Unlike the NT-hp, this mutation abrogates helicase activity completely. The double mutant with mutations on both the NT-hp and the PS1-hp has lost DNA binding (McGeoch *et al.*, 2005). Thus, these two hairpins are vital for interacting with DNA in the channel, while the PS1-hp within the helicase domain has an additional and more direct impact on helicase activity. Interestingly, the hairpin in SV40 LTag equivalent to MCM PS1-hp extends into the central channel and is shown to move large distances within the channel in response to ATP binding/hydrolysis, likely to provide a "power stroke" for DNA unwinding (Li *et al.*, 2003; Gai *et al.*, 2004b). However, the PS1-hp in ssoMCM is recessed from the central channel and resides close to the side channel in our hexamer structure model (Brewster *et al.*, 2008). Whether this β-hairpin of ssoMCM will move to the main channel upon ATP binding, like LTag, will need to be determined by future X-ray studies with nucleotides.

Two other hairpins present in the C-terminus include the H2I-hp and the EXT-hp (Figures 1A, 1C and 1D; Brewster *et al.*, 2008). The H2I-hp is a β-hairpin insertion into helix 2 of the C-domain that projects directly into the central channel, with the tip of the β-hairpin carrying a small 3_{10}-like helix that appears to present a steric block in the central channel (Brewster *et al.*, 2008). The central channel location of this structural element is predicted based on EM studies (Jenkinson and Chong, 2006; Costa *et al.*, 2006a). Deletion of residues within the H2I-hp greatly enhances ssDNA and dsDNA binding, but eliminates helicase activity (Jenkinson and Chong, 2006). Further, the ATPase activity of this mutant is not affected by the absence or presence of ssDNA, but was stimulated 12-fold by the addition of dsDNA. These data led to the proposition that this hairpin may act as a "plowshare" to separate the two DNA strands during unwinding (see below) (Jenkinson and Chong, 2006).

The EXT-hp (not present in mkaMCM2) is peculiarly situated near the side channel exit on the exterior side of the hexamer model of ssoMCM. A triple mutation on the tip of the EXT-hp (E326A/D327A/R329A) compromises helicase activity, suggesting the importance of this EXT-hp for DNA unwinding in MCM (Brewster *et al.*, 2008). Our recent biochemical analysis also suggests that this hairpin is involved in DNA binding (Brewster *et al.*, submitted).

Assaying MCM helicase activity

Before going into the details regarding the unwinding models, we will comment briefly on the large amount of biochemical and helicase studies available in the literature. Normally, small, synthetic DNA substrates are used in helicase studies. These substrates are typically two oligonucleotide primers with complementary regions annealed together to produce small, forked, Y-shaped DNAs, or overhang DNAs. One strand is radio-labeled,

and assays are performed *in vitro* with purified helicase, with the unwound products analyzed by poly-acrylamide gel electrophoresis. It is important to note that the synthetic forked and overhang substrates used in most helicase assays (including ours) should not be biologically relevant. Forked substrates with single stranded ends presumably do not form during melting at the origin *in vivo*. The free single stranded DNA ends available in *in vitro* assays may allow the hexameric helicase ring to latch onto a ssDNA overhang and translocate along the ssDNA to displace the complementary strand, resulting in unwound ssDNA products. In this sense, a forked DNA unwinding assay is similar to a translocation assay.

An *in vitro* unwinding assay system that can initiate melting and unwinding from an origin sequence in the middle of a blunt-ended dsDNA substrate would likely mimic the unwinding mode that is most closely related to *in vivo* DNA replication. While no such assay system is available for MCM yet, SV40 LTag can robustly unwind blunt ended dsDNA with an origin sequence in the middle (Bullock, 1997). Also, the recent progress in being able to assemble a double hexamer of scMCM on dsDNA may very well render such an assay system feasible for MCM in the future (Remus *et al.*, 2009). For this reason, it seems that the helicase data collected so far for eukaryotic and archael hexameric or double-hexameric helicases should be viewed with caution.

Oligomerization of MCM

While it is well accepted that MCM forms hexameric complexes, it is unclear if MCMs from different organisms will form double hexamers. Interestingly, some parallels exist between what is already observed for SV40 LTag and MCM. Currently, there is a large amount of evidence supporting a double hexamer as the active helicase for SV40 LTag for viral DNA replication (see Sclafani *et al.*, 2004 and references therein). Further, double hexamerization of LTag greatly stimulates helicase activity (Smelkova and Borowiec, 1998; Alexandrov *et al.*, 2002), and is generally important for viral DNA replication (Mastrangelo *et al.*, 1989; Smelkova and Borowiec, 1997; Simmons, 2000). As SV40 relies on cellular co-factors, it is conceivable that the process used by LTag would mimic that of MCM in eukaryotic cells. In eukaryotes, the hexamer composed of two MCM4, 6 and 7 trimers has also been shown to be more processive as a double hexamer than a hexamer, although it is unclear whether the two hexamers were in a head-to-head configuration in that report (Lee and Hurwitz, 2001).

While much less is known about the active form of the MCM helicase during genomic replication in archaea and eukaryotes, crystal structure and EM studies from our group and others reveal a double hexamer architecture for mthMCM (Fletcher *et al.*, 2003; 2005; Gómez-Llorente *et al.*, 2005; Costa *et al.*, 2006b). Further, recent work has established that the MCMs from *Saccharomyces cerevisiae* (scMCM) are loaded as a double hexamer onto origin dsDNA (Remus *et al.*, 2009). These emerging data in archaea and eukaryotes may suggest a unified theme for a functional double hexamer *in vivo*, despite the fact that details describing how a double hexamer works to unwind two replication forks bi-directionally still remain largely unknown (Sclafani *et al.*, 2004).

SsoMCM has so far been mainly reported as hexamers (Carpentieri *et al.*, 2002), with a hint of evidence indicating larger oligomers, some of which may contain double hexamers (Barry *et al.*, 2007). We also have some data indicating ssoMCM double hexamerization may be salt dependent (Brewster *et al.*, unpublished data), and it has been recently shown this is the case for mthMCM (Shin *et al.*, 2009) (discussed more below). Thus, double hexamerization of archaeal MCM may be dependent on local conditions.

Double hexamerization of mthMCM is well studied, by X-ray crystallography (Fletcher *et al.*, 2003) and by cryo-EM, where sample conditions were in the presence and absence of DNA. MthMCM's N-domains come together in a "head to head" configuration (Fletcher *et al.*, 2005; Gómez-Llorente *et al.*, 2005; Costa *et al.*, 2006b). This double hexamerization appears to affect helicase activity *in vitro*, because the mutation of an N-terminal arginine (R161A) at the double hexamer interface prevents formation of double hexamers and weakens helicase activity, especially at lower protein concentrations (Fletcher *et al.*, 2005). This is reminiscent of the case in SV40 large T antigen, where the double hexamer has ~10–15 fold higher helicase activity than the single hexamer (Smelkova and Borowiec, 1997). However, a recent report shows that mthMCM's oligomerization state is dependant on the concentration of salt and protein in the absence of nucleotide and DNA (Shin *et al.*, 2009). They found that lower protein concentrations yield more monomers, higher concentrations favor hexamers, and even higher concentrations favor double hexamers. Further, helicase activity was shown to be inhibited at high concentrations, as was noted previously for mthMCM (Fletcher *et al.*, 2005), for the viral replicative helicase SV40 LTag (Gai *et al.*, 2004a) and as we have seen for ssoMCM (unpublished data). Importantly, they found optimal activity at concentrations sufficient to form a hexamer. Higher concentrations conducive to double-hexamerization were inhibitory.

Next they analyzed the activity of the R161A mutation versus protein concentration. In contrast to our report, they found that activity of single hexamers did not fall off as concentration increased. The source of

this contradiction is unknown, but it seems likely that helicase activity is affected by oligomerization state, and potentially experimental conditions. Perhaps the above note regarding the relevance of forked DNA substrates is applicable, but clearly future experiments are needed to provide illuminating insights into these seemingly conflicting results.

A parallel to LTag is applicable here. *In vitro* conditions can drive double hexamerization of LTag or inhibit it, and this in turn can change fork topology during unwinding. Electron microscopy data of LTag–dsDNA unwinding complex shows a population of "rabbit ear" structures indicative of bidirectional fork unwinding localized to a single double-hexamer (or dodecameric) complex (Wessel *et al.*, 1992). The population of these double loop structures versus two-fork bubble structures can be changed depending on the assay conditions. For example, a monoclonal antibody was added that theoretically bound to both hexamers. It was argued this stabilized the double hexamer, and correspondingly it raised the population of rabbit ear loops. Conversely, incubating with ETDA decreased the population. *In vivo*, the local conditions are unknown; the double hexamer may be destabilized, or there could exist bridging co-factors to stabilize double hexamerization. If local conditions can change LTag's fork topology, perhaps they can alter that of mthMCM as well.

Whether MCM operates as a single or double hexamer *in vivo* directly affects how DNA replication is organized in the cell (reviewed in Cook, 1999; Sclafani *et al.*, 2004; Takahashi *et al.*, 2005; Sakakibara *et al.*, 2009). A single hexamer model often leads to the idea that two replication forks travel away from each other, creating a bubble centered on the origin of replication. In this model, the DNA would be stationary and large replication machinery, including a large body of co-factors, accessory clamps, primase and polymerase, would travel along the DNA. An alternate model is the stationary factory model. Rather than a large replication protein complex moving along the DNA, the chromosomal DNA would be pulled into a replication complex that may be anchored on the nucleo-matrix. Currently, evidence is building that the latter model of stationary factories is the favored *in vivo* model (Cook, 1999; Anachkova *et al.*, 2005). If the MCM helicase operates as a double hexamer, the two growing replication forks would be held close to each other by the helicase, which could act as an anchoring platform for assembling other replication proteins on the growing forks. This would necessitate a factory model; and the traveling model would not be possible. We note, however, the converse is not true; a factory model does not necessitate double hexamerization. Two single hexamers connected through other factors in a factory is also conceivable.

Possible models of DNA unwinding by the single hexamer

While it is still in debate which hexameric state is the biologically active form for cellular DNA replication *in vivo*, it is clear that a single hexamer of MCM, as well as LTag, can unwind DNA substrates with 3′-end ssDNA overhangs in *in vitro* assays (Ishimi, 1997; Morris *et al.*, 2002). This is similar to the case for the DnaB family helicases in prokaryotic cells and phages, which require a 5′-end ssDNA overhang to unwind the dsDNA substrate (reviewed in Patel and Picha, 2000; Donmez and Patel, 2006)). In this regard, substantial biochemical evidence has been gathered indicating probable sites of DNA interaction in ssoMCM and mthMCM (outlined below), which can help elaborate models for MCM–DNA interactions during unwinding using dsDNA substrates with ssDNA available as a 3′-overhang. Currently, there are several unwinding models that are proposed for MCM as a single hexamer: the steric exclusion model, the rotary pump model, the strand extrusion model, and the plowshare model.

Steric exclusion

Steric exclusion is proposed as the unwinding mechanism for DnaB family helicases in prokaryotes, which likely work as a single hexamer for genomic DNA replication (Patel and Picha, 2000). In this model, a hexameric helicase encircles and translocates along ssDNA towards the fork, unwinding the DNA fork by excluding the opposite strand from the hexamer (Figure 2C). The MCM 4, 6, 7 hexamer has been shown to use this mechanism on synthetic fork substrates *in vitro* (Kaplan *et al.*, 2003). Further, FRET data seems to show that the 5′ tail in a forked substrate dynamically interacts with the exterior of the ssoMCM protein, rapidly binding and unbinding during unwinding (Rothenberg *et al.*, 2007).

The viral E1 helicase ssDNA-bound crystal structure also indicates steric exclusion may be one of the unwinding mechanisms for E1 (Enemark and Joshua-Tor, 2006). Recent debate surrounding E1 and LTag mechanisms has centered on whether LTag double hexamerization is relevant to its biological function, meaning whether the rabbit-ear structures observed by *in vitro* EM represent the *in vivo* unwinding mechanism (as discussed earlier) (Wessel *et al.*, 1992). It is argued that the E1 crystal structure with ssDNA bound suggests a possible steric exclusion mode (Enemark and Joshua-Tor, 2006; 2008), which should be extended to other hexameric helicases. It is further argued the central channel of LTag is too small to accommodate dsDNA. We have contended that LTag's central channel can accommodate dsDNA (Li *et al.*, 2003), as suggested by EM studies and biochemistry studies (reviewed in Fanning

and Zhao, 2009). Additionally, as noted above, there is also strong evidence that LTag double-hexamerization is relevant *in vivo*. We await a DNA-bound LTag structure to help resolve the question, but note it is possible that the enzymes can have multiple modes of unwinding depending on whether a single or a double hexamer is at work and depending on if it is operating *in vitro* or *in vivo*. Of course, available evidence does not exclude the possibility that these enzymes may simply operate by different means.

Rotary pump

Another model is the rotary pump, wherein many single hexamers bind at an origin, spread out along the chromosome, then are anchored in place and rotate DNA – thus, introducing negative supercoiling to unwind it (Laskey and Madine, 2003; Takahashi *et al.*, 2005; Sakakibara *et al.*, 2009). This model is proposed partially based on the observation that large numbers of excess MCM are loaded during replication on the chromosome (reviewed in Forsburg, 2004). Considering the large number of replication proteins and chromosomal associated proteins bound to the DNA, it would require large-scale coordination between these proteins for this mechanism to work.

Strand extrusion and plowshare

Analysis of DNA binding in the different regions of the hexamer suggests a change from double to single stranded DNA occurs at a point buried in the central channel of the enzyme. If such a change occurs, it seems likely the two single strands would emerge from the enzyme from different pores, leading to the strand extrusion model (Figure 2G). The evidence comes from two reports which analyzed DNA binding to ssoMCM mutants consisting of only the N- or C-domains. The first report found that N-ssoMCM binds ssDNA with an affinity at least comparable to wild type but that C-terminal ssoMCM (C-ssoMCM) has greatly compromised ssDNA binding (Pucci *et al.*, 2007). The second report found that C-ssoMCM can bind dsDNA with good affinity (and in a highly cooperative manner), but N-ssoMCM cannot (Liu *et al.*, 2008). The N-ssoMCM structure bears this out, as the central channel seems too narrow to encircle dsDNA (Liu *et al.*, 2008). However, the N-terminal double hexamer of mthMCM clearly can bind dsDNA and ssDNA (Fletcher *et al.*, 2003). Interestingly, an EM study of mthMCM in the presence of dsDNA reveals dsDNA in the channel bound to one of the hexamers in the double hexamer, and possibly only in the C-domain (Costa *et al.*, 2006a). Together these data all seem to indicate that the hexamer can accommodate both dsDNA and ssDNA in the C-domain and the N-domain, but may possess a preference for dsDNA in the C-domain and for ssDNA in the N-domain. During DNA unwinding by a single hexamer, if the C-domain binds dsDNA and the N-domain binds ssDNA, then the other ssDNA strand may be extruded between the two domains through one of the six side channels near the ATP binding site. The other strand would continue in the central channel and exit through the N-terminal central channel. Some of the earliest work on archaeal MCMs found that the ssDNA binding site and the ATP binding site may overlap (Chong *et al.*, 2000). This could be due to conformational shifts upon ATP binding directly affecting ssDNA affinity. However, it may also be due to the proximity of the ATP binding site to the side channel that may serve to passage ssDNA.

Extruding both strands out of two side channels (Figure 2E) could be an alternative unwinding mode. However, this model does not seem to agree with the findings that the interaction of the N-terminal NT-hp with DNA is important for helicase activity (Fletcher *et al.*, 2003; McGeoch *et al.*, 2005). At this moment, it requires further investigation as to whether this interaction of NT-hp with DNA is important only for the initial DNA binding at the beginning of unwinding or critical during unwinding as well.

A previously proposed model for DNA unwinding by a rigid motif, the "plowshare" (Takahashi *et al.*, 2005), can be adapted to the strand exclusion model. The plowshare was thought to be at the end of a single hexamer with respect to the direction of dsDNA movement and would be dragged behind the hexamer as it translocated on dsDNA, splitting the two strands during the translocation process in a manner similar to the RecBCD pin (Singleton *et al.*, 2004; Takahashi *et al.*, 2005). Such a pin is not present at the exit of the central channel in our ssoMCM hexamer structure model. While the NT-hp is situated near a likely DNA exit pore (the N-domain central channel), it is dispensable for helicase activity (McGeoch *et al.*, 2005; Barry *et al.*, 2009). An element of the C-terminal winged helix domain could be a candidate; however its deletion results in higher ATPase and helicase activity (Barry *et al.*, 2007). Thus, the most reasonable proposal is that the H2I-hp in the middle of the channel fills the role of the plowshare (Jenkinson and Chong, 2006). The presence and location of the H2I-hp is confirmed in the crystal structure of the near-full-length ssoMCM (Brewster *et al.*, 2008).

Further supporting side channel utilization, the crystal structure reveals an unexpected (acidic) EXT-hp that is situated on the exterior of the protein near the side-channel, not at the central channel. It is intriguing that EXT-hp is critical for ssoMCM helicase function (Brewster *et al.*, 2008), and involved in DNA binding (Brewster *et al.*, submitted). This suggests that the side-channel may be used for DNA unwinding, possibly for

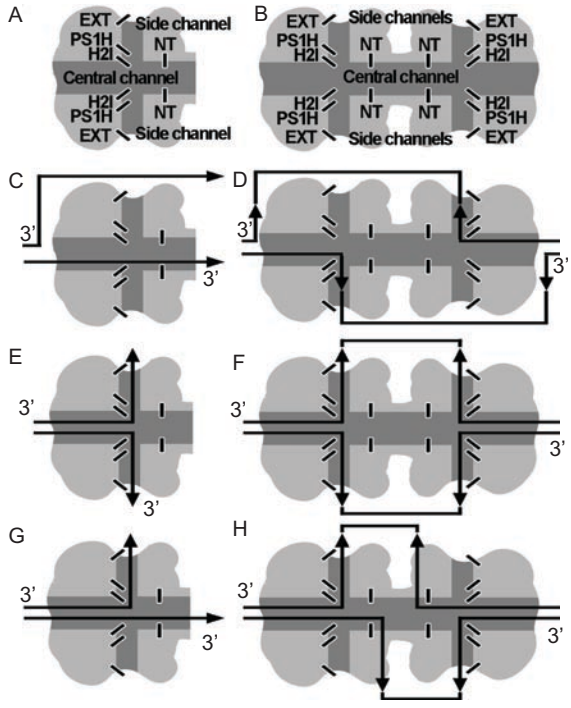

Figure 2. Possible DNA unwinding modes by MCM helicase. (A), (B) Schematic representation of MCM helicase as a hexamer (A) or double hexamer (B). The four β-hairpins (NT, H2I, PS1, and EXT hairpins) are represented by short solid bars; the central channel and the side channels are in darker shades. (C), (D) Steric exclusion model for a single hexameric (C) or double hexameric (D) MCM helicase. (E) Double side extrusion model, showing ssDNA exiting from two different side channels. (F) Double side extrusion model adapted to a double hexamer becomes the looping model. (G) Single side-channel extrusion model, showing one ssDNA strand extruding from a single side channel, while the other ssDNA strand remaining in the central channel. (H) Asymmetric looping model, ssDNA is extruded from N- and C- terminal side channels. DNA is shown as black lines. Arrows indicate direction of DNA translocation movement. Figure and caption adapted from (Brewster *et al.*, 2008).

direct ssDNA binding, as shown in model Figure 2G. The exact mechanism for the involvement of this EXT-hp in DNA unwinding is worth further investigation.

The model in Figure 2G is attractive in that it satisfies all of the DNA binding data discussed above, including the encircling of dsDNA by MCM that likely is biologically relevant (reviewed in Takahashi *et al.*, 2005), and the involvement of each of the four hairpins in binding DNA (see discussion below). However, it runs afoul of an unwinding result obtained *in vitro*, in which MCM 4, 6, 7 heterohexamer cannot unwind forked substrate with a biotin/streptavidin block on the middle of the 3′→5′ strand, but it can unwind substrate with a block on the 5′→3′ strand (Kaplan *et al.*, 2003). This result argues for the strand exclusion model in Figure 2C: MCM can bind the 3′ end of a forked substrate and translocate on it, unwinding the other strand, as long as there is no block on the 3′ strand. Because the 5′ strand is excluded in this model, a block is permissible on that strand as the block would not enter the central channel. Clearly more data are needed to resolve the issue.

Models of DNA unwinding by the double hexamer

As discussed above, various structural and biological data suggest that SV40 LTag works as a double hexamer for viral DNA replication *in vivo*, and available evidence also suggests that MCM may function as a double hexamer. If these ring-shaped helicases function as a double hexamer to unwind two replication forks bi-directionally, how do the two DNA forks propagate and how are they organized by the double hexamer? We present several hypothetical models and discuss how they fit the present body of research data.

Steric exclusion

Simply expanding the model for a single hexamer in Figure 2C to a double hexamer is impossible, as it would lead to non-complementary ssDNA strands sliding across one another in the N-terminal central channel. However, if a side channel is utilized for the ssDNA exit so that the N-domain no longer binds DNA (Figure 2D), then the steric exclusion model can be adapted to a double hexamer. Interestingly, this satisfies many of the observations made above with regards to the single hexameric strand extrusion model, but it does not engage the NT-hairpin. However, in this model, the NT-hp could be utilized during initial melting and/or loading of the complex. This is seen in *S. cerevisiae* MCM5; a triple mutant on the NT-hp affects replication initiation and origin binding (Leon *et al.*, 2008; Bochman and Schwacha, 2009). It also suggests a different role for the H2I-hp than a plowshare: as the deletion of the H2I-hp increases DNA binding (Jenkinson and Chong, 2006), perhaps it serves to direct DNA in the central channel towards a side channel, where it is picked up by the PS1-hp and extruded.

Looping models

A double looping model (Figure 2F) has been proposed for LTag previously (Li *et al.*, 2003; Gai *et al.*, 2004b). This looping model can be directly extended from the unwinding model for a single hexamer shown in Figure 2E. Again, the NT-hp is not utilized for DNA unwinding, but perhaps initial N-terminal DNA binding is necessary for establishing unwinding conformation, with DNA relocating to the side-channel after initiation and conformational rearrangement. Because the AAA+ helicase domain alone of ssoMCM showed

helicase activity (Barry *et al.*, 2007), this suggests that the N-domain is dispensable for unwinding, which is consistent with this model. However, evidence also seems to suggest that dsDNA and/or ssDNA interactions within the N-terminal central channel are important for mthMCM beyond initiation (Fletcher *et al.*, 2003; McGeoch *et al.*, 2005). More investigation will be needed to understand the N-terminal role in DNA unwinding *in vitro* and *in vivo,* however we discuss below the possibilities arising from the presence of either dsDNA or ssDNA in the N-terminal channel.

If dsDNA moves through the N-domain of one of the two hexamers during unwinding, then an odd situation of a double hexamer unwinding a single replication fork arises (model not shown). It is noteworthy that mthMCM EM models bound to dsDNA show an asymmetry lengthwise through the double hexamer (Costa *et al.*, 2006a). One possibility is that one hexamer translocates on dsDNA in front of the DNA fork while the other hexamer at the fork separates it and extrudes ssDNA, leading to asymmetry in the structure. In this case, instead of two single hexamers moving at two forks, or one stationary double hexamer holding two separate forks together, there would be two double hexamers, possibly mobile, each with a single fork. However, given the double hexamer architecture observed in SV40 large T, archaeal MCM, and eukaryotic MCM (Valle *et al.*, 2006, Gómez-Llorente *et al.*, 2005, Remus *et al.*, 2009), the model of one double hexamer on one replication fork is less likely, although we cannot exclude it. We note here that recent work has shown that eukaryotic MCM double hexamers can at least "slide" along dsDNA (Remus *et al.*, 2009).

If ssDNA moves through the N-domain, as proposed during unwinding for a single hexamer shown in Figure 2G, it can be easily adapted to unwinding by a double hexamer (Figure 2H). ssDNA would pass through part of the central channel and then loop out from N- and C-domain side channels observed in crystal structures of N-mthMCM, as well as in the hexamer model of ssoMCM (Fletcher *et al.*, 2003; Brewster *et al.*, 2008). This model is reminiscent of past asymmetric looping models proposed or SV40 large T (Gai *et al.*, 2004b; Valle *et al.*, 2006). Here, one DNA strand is extruded out of a C-terminal side channel, and the other is extruded out of a putative N-terminal secondary side channel. Secondary N-terminal side channels can be visualized in the EM structure of double hexameric LTag (Valle *et al.*, 2006). Further, these channels are also visible in mthMCM EM maps (Pape *et al.*, 2003) (Figures 3A and 3B), and the recent eukaryotic EM MCM map (Remus *et al.*, 2009). Additionally, they are also visible in the N-mthMCM double hexamer structure (Figure 3C), and the hexamer model generated from the X-ray structure of ssoMCM. While this channel can, in principle, allow ssDNA passage, we stress that whether it could be used as an ssDNA exit is highly hypothetical at this stage. In this model, both C-terminal central channels contain dsDNA, both N-terminal central channels contain ssDNA, and all the functionally important structural motifs in the ssoMCM structure are engaged. As such,

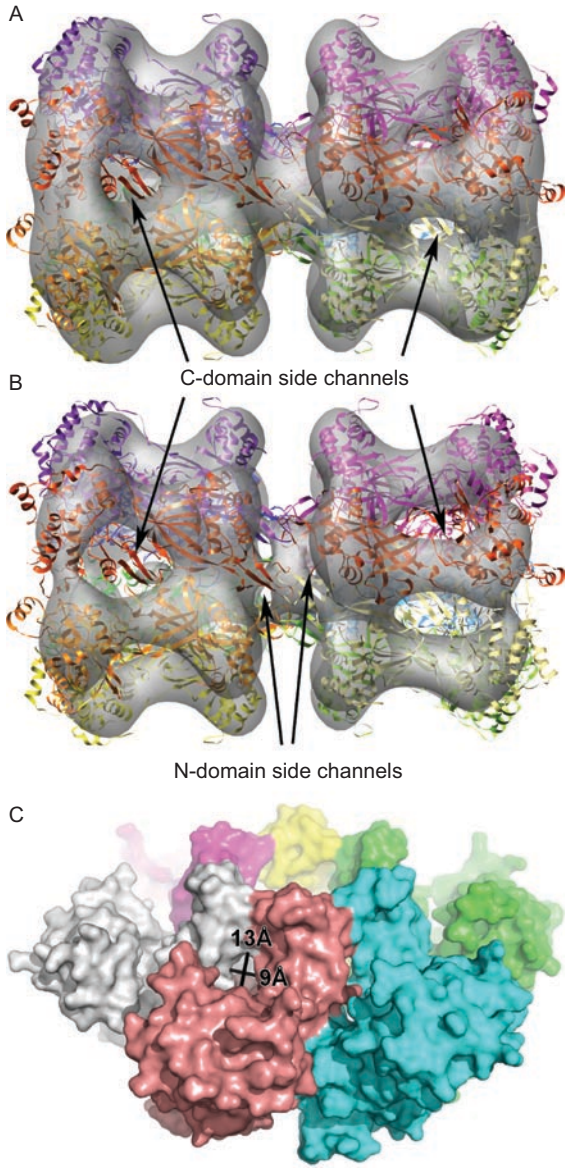

Figure 3. The side channels at the C-domain and N-domains. (A) Electron-microscopy map of double hexamer mthMCM (Gómez-Llorente *et al.*, 2005) in which a double hexamer model of ssoMCM fits. (B) The EM map shown in panel A, but with a higher threshold. The visible side channels in the N- and C- domains are indicated. (C) Space filling model of N-mthMCM with N-terminal side channel measurements indicated (Fletcher *et al.*, 2003). Note, the N-ssoMCM space-filling model (Liu *et al.*, 2008) does not show these gaps, but its zinc binding domain is substantially shifted compared to either the N-mthMCM structure (Fletcher *et al.*, 2003) or the near full-length ssoMCM structure (Brewster *et al.*, 2008).

this unwinding model by a double hexamer seems to satisfy the structural and DNA binding data the most.

Detailed structural features for DNA unwinding

The ATP bound structure of LTag reveals a tight ATP binding pocket, with key residues bonding with the ATP from both the cis- and trans- side (Gai *et al.*, 2004b) (Figures 4, 5). In the ssoMCM hexamer model, key trans- residues (such as the arginine finger) are within a reasonable distance, but are more recessed from the pocket, similar to, but to a greater extent than, the apo LTag hexamer structure (Brewster *et al.*, 2008; Gai *et al.*, 2004b). Recent work established that a residue at the base of the EXT-hp, R331, is critical for ATPase and helicase activity (Moreau *et al.*, 2007).

It is possible that this residue has an analog in the LTag binding pocket. In the sequence alignments of AAA+ ATPases including ssoMCM and LTag, a stretch of 11 amino acids in ssoMCM or five amino acids in LTag in the C-domain do not align in the majority of the AAA+ ATPases (Figure 5A) (Iyer *et al.*, 2004). In ssoMCM, these 11 amino acids are the EXT-hp (residues 321–331). In LTag, the five amino acids form a small loop (residues 413–417, Figure 5B). It appears that ssoMCM R331 may align structurally with LTag K418. LTag's K418 has been identified as a "lysine finger" that works with the arginine finger to coordinate the ATP gamma phosphate (Li *et al.*, 2003; Gai *et al.*, 2004b). Mutation of LTag K418 to alanine abrogates both ATPase and helicase activity (Greenleaf *et al.*, 2008).

Adjacent to LTag K418 is another lysine, K419, that is also involved in ATP hydrolysis (Figure 5B). LTag K419 interacts with the ribose in the ATP bound structure (Gai *et al.*, 2004b), and has a much less severe phenotype than K418 (Greenleaf et al., 2008). Our triple mutant that included ssoMCM R329 also had a less severe phenotype than was reported for ssoMCM R331 (Brewster *et al.*, 2008; Moreau *et al.*, 2007). While the k_{cat} remained unchanged, the k_m for binding was significantly affected, and in the presence of Y-DNA, the k_m was high enough to make the k_{cat} immeasurable. We have preliminary data for the R329 mutant alone that shows a reduction, but not elimination, of ATPase activity (Brewster *et al.*, submitted). Thus, the phenotypes suggest that ssoMCM R331 is equivalent to LTag lysine finger K418, and ssoMCM R329 is equivalent to LTag K419. This hypothesis requires further verification with a structure of ssoMCM hexamer bound to nucleotide.

In the ssoMCM hexamer model, we measured the main chain–main chain distance of R331 ("lysine" finger) to K346 (Walker A) in angstroms. This "pocket distance" was compared to the pocket distance of LTag (between equivalent LTag residues K418 and K432), in both ATP bound and apo forms (Figures 5C and 5D). The LTag ATP bound pocket distance is 12.6 angstroms compared to its apo distance of 18.4 angstroms. The ssoMCM hexamer model has a pocket distance of 26.6 angstroms, which seems excessively large for a residue that needs to interact with the ATP. If these two residues are directly interacting with the ATP, it seems they need to close a 14 angstrom gap first.

Similarly, LTag's arginine finger moves in response to ATP binding, from 20.4 angstroms to 14.7. The ssoMCM distance is 16.9 angstroms, indicating the gap is much less severe for this residue (only 2.2 angstroms instead of 14). Thus, we will focus on the R331-K346 pocket distance.

Based on the discussion above and comparison with what is known about SV40 LTag, we propose a mechanism for conformational changes of ssoMCM in response to the ATP binding cycle, which can probably couple the movement of the β-hairpins for DNA unwinding and translocation. First, ATP binding on the p-loop will bring R331 on the EXT-hp of a neighboring monomer close to

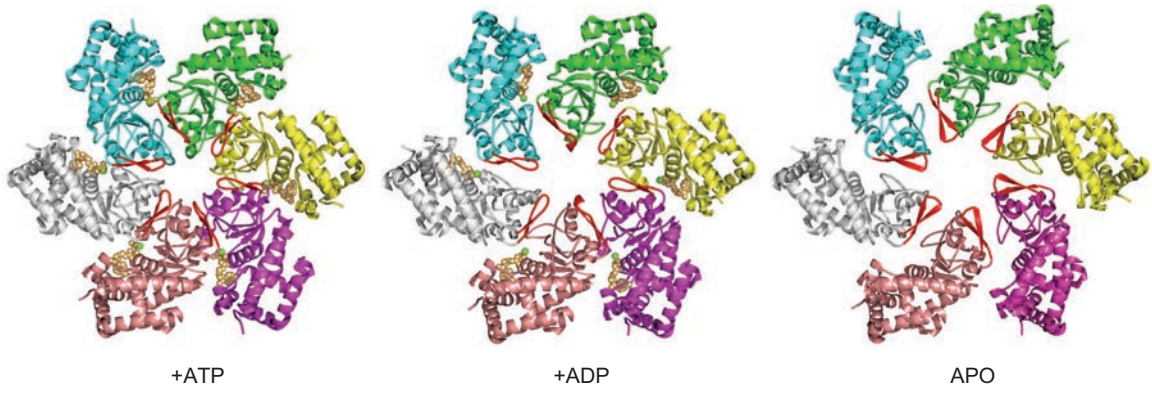

Figure 4. Overview of LTag hexamer conformations and the β-hairpin structure in different nucleotide binding states. Three nucleotide binding states of LTag hexameric helicase, seen from above (N-terminal face). Monomers are colored, with their central β-hairpins in red (equivalent to the PS1-hp of ssoMCM). The N-domain, D1, has been removed for clarity. Adapted from Gai *et al.* (2004b).

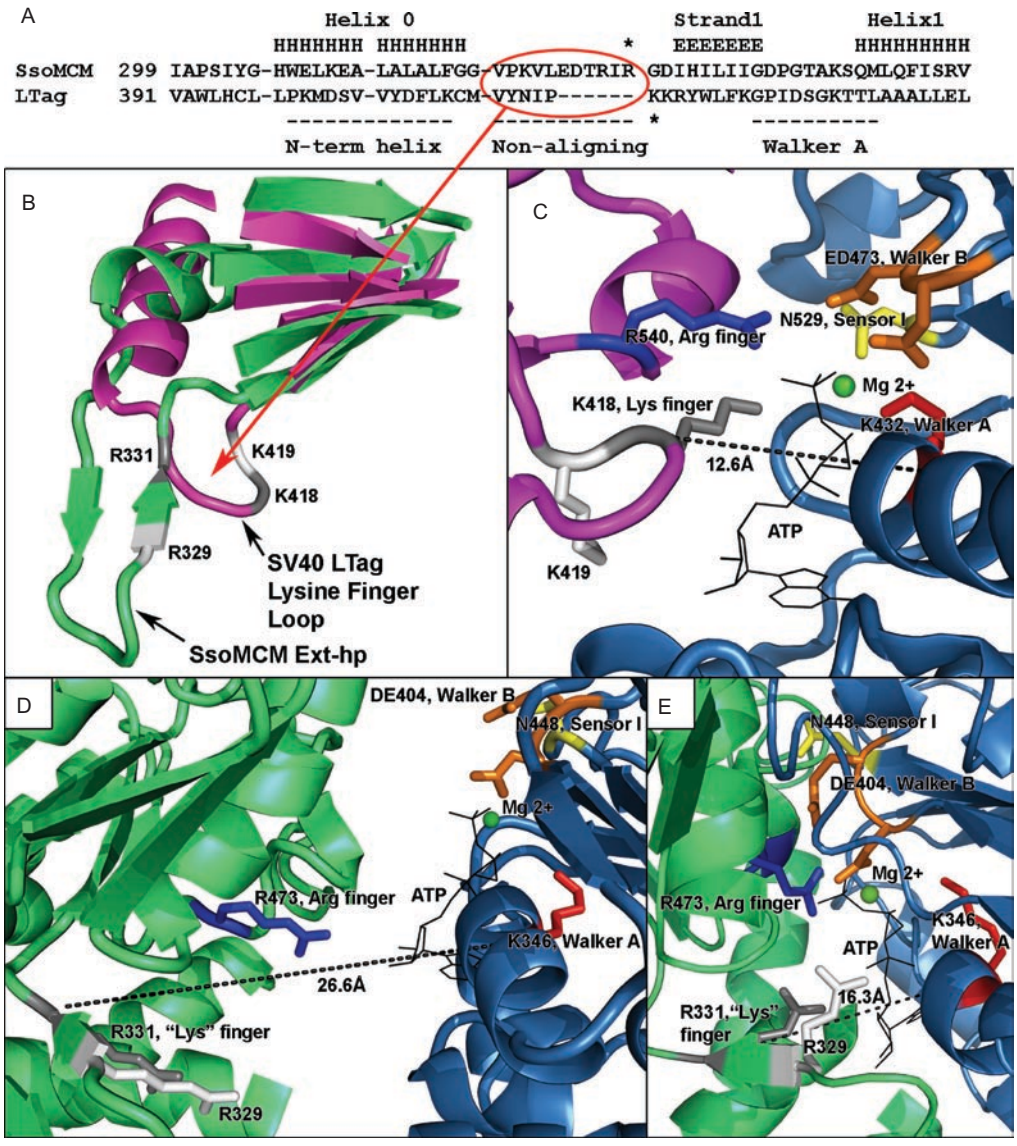

Figure 5. The nucleotide pocket configurations in LTag and SsoMCM. (A) The sequence alignment between ssoMCM and LTag around the EXT-hp of ssoMCM, adapted from (Iyer *et al.*, 2004). Secondary structure is listed above (H: helix, E: strand). The circled region is an 11-amino acid (AA) region (ssoMCM) or a 5-AA region (SV40 LTag) that is not conserved among AAA+ ATPases. This region corresponds to the Ext-hp (ssoMCM) or a small loop in LTag that houses its lysine finger (K418). The * indicates ssoMCM R331 (top sequence). Another * indicates LTag K418 (lower sequence). (B) Structural alignment of a portion of ssoMCM (green), and LTag (magenta). The five-strand β-sheet from the AAA+ ATPase core is in the upper right; helix 0 from the C-domain is in the upper left. Residues which may have functional equivalence are colored the same (such as ssoMCM R331 and LTag K418 in gray). (C) LTag ATP binding pocket, with an ATP bound. Cis- residues (named such due to residence on the monomer presenting the p-loop) are on the right, from the blue monomer; trans- residues are on the left, from the magenta monomer. The nucleotide pocket distance is indicated, measured from K418 to K432 (main-chain to main-chain). (D) SsoMCM nucleotide pocket from the hexamer model. The pocket distance is measured from R331 to K346. Amino acid side chains and the ATP position are modelled in. (E) A simulated ssoMCM closed ATP binding pocket. Amino acid side chains and the ATP are modeled in to approach the ATP without altering the protein backbone.

the ATP/p-loop to make bonding contacts, closing the gap between the two monomers, and leading to the shift and rotation of the C-terminal AAA+ domain relative to the N-domain, very much like the iris-movement observed in the SV40 LTag in response to ATP binding cycle (Figures 4 and 6) (Gai *et al.*, 2004b). The N- and C-domains have been shown to operate independently; separately purified N- and C- terminal ssoMCM mixed together have stimulated helicase activity compared to the C-terminal alone (Barry *et al.*, 2007). This domain shift and rotation of the AAA+ domain should also lead to the coordinated movement of the three β-hairpins in the main and side channels, which can be coupled with DNA translocation and remodeling (Figure 6). A movie simulating such conformational changes is shown as part of the Figure 6 supplement.

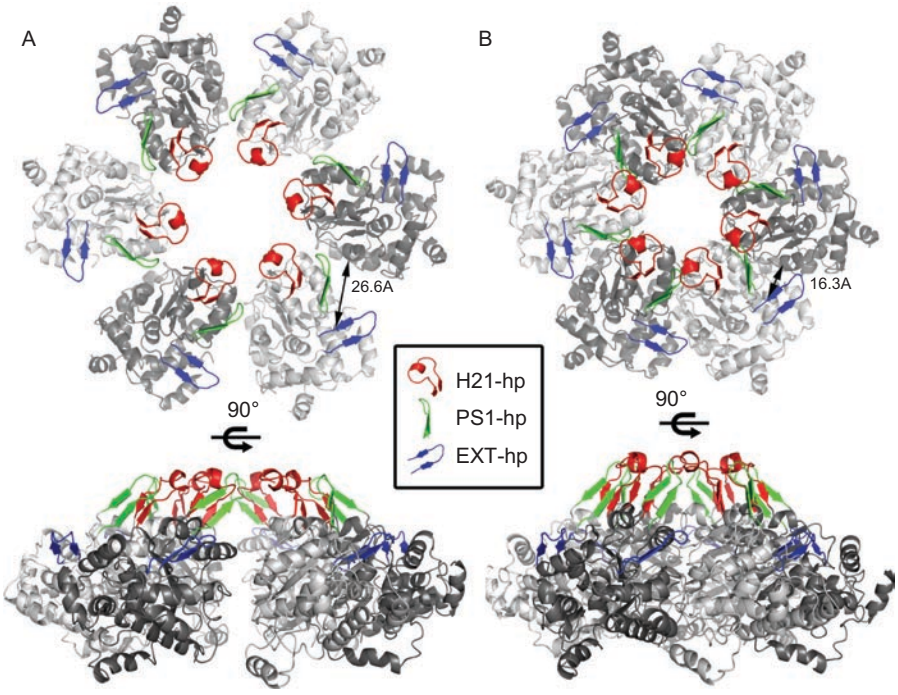

Figure 6. Nucleotide pocket closure in ssoMCM and the conformational changes of the hexamer. (A) Top and side views of the ssoMCM hexamer model in the absence of nucleotide binding (Brewster *et al.*, 2008). The N-domain and some surface loops are hidden for clarity. The three C-terminal β-hairpins are colored. Red: helix-2 insert hairpin (H2I-hp). Green: pre-sensor 1 hairpin (PS1-hp). Blue: exterior hairpin (EXT-hp). The main-chain to main-chain distance from the EXT-hp residue R331 ("lysine" finger) to the Walker A residue K346 is shown in angstroms (the pocket distance). (B) Same orientations shown as in panel A, but with simulated nucleotide pocket closure triggered by ATP binding, resulting in the rotations and a translation of the C- domain of each monomer. See text for details.

Potential roles of the β-hairpins in DNA unwinding

In the simulation of the conformational changes triggered by ATP binding shown in Figure 6, we modeled the tightening of the ATP binding pocket through a series of five steps. The final pocket distance (R331 to K346) after these movements is 16.3 angstroms. The arginine finger distance narrowed to 13.7 angstroms. The end result of these movements is a tightening of the central channel, and an upward movement (toward the N-terminus) of the PS1-hp and H2I-hp. These results parallel the tightening of the LTag hexamer upon ATP binding (Figure 4) (Gai *et al.*, 2004b).

The PS1-hp, required for helicase activity and involved in DNA binding in MCM and LTag, lies recessed from the central channel in our hexamer model of ssoMCM. In our simulation, closing the ATP pocket upon ATP binding seems to move the PS1-hp further into the channel and up toward the N-terminus. If movement of this β-hairpin into the central channel upon ATP binding facilitates DNA binding, then perhaps hydrolysis of ATP would restore the PS1-hp closer to the side channel, which could move separated ssDNA with it and promote ssDNA extrusion through the side channel. Further, this movement could cause a shift of the NT-hairpin, mediated through the ACL, facilitating the C- to N-domain communication seen previously (Sakakibara *et al.*, 2008; Barry *et al.*, 2009). Indeed, it was reported that the distance between the ACL and the PS1-hp (in trans-) increases when ATP is bound (Barry *et al.*, 2009), which is supported by our modeling result.

The hexamer model of ssoMCM shows that the H2I-hp extends away from core subunit structure and protrudes into the central channel (Brewster *et al.*, 2008). Further, the H2I-hp lies between two side channels and under the NT-hp of an adjacent subunit, forming a helical arrangement of hairpins within the central channel (Figure 1C, 1D). The simulation suggests that ATP pocket closure through ATP binding may recess the H2I-hp away from central channel as the PS1-hp projects further into it. ATP hydrolysis and release would restore the H2I-hp to the central channel, which could split new base pairs along dsDNA. In this sense, it may act as a structural element to insert into the dsDNA between strands in a plowshare manner as discussed above. Indeed, while the H2I-hp itself is conserved, poor sequence conservation within the H2I-hp has led to the idea that its interactions are non-amino acid specific, presumably steric (Jenkinson and Chong, 2006). We note, however, that

this hypothesis would carry more weight if the H2I-hp projected further into the central channel in the apo hexamer model.

FRET data shows the 5′ tail of a forked DNA substrate binding and releasing to the hexamer dynamically during unwinding, presumably to the exterior (Rothenberg *et al.*, 2007). The EXT-hp could be in a place suited to disengage the 5′ strand from the exterior of the protein. This could be accomplished through its hydrophobic and acidic tip (VLED, 324–327), leaving R329 and R331 to be involved in ATP hydrolysis only. However, our newly obtained analysis of this hairpin shows E326, D327, R329 and R331 are all involved in DNA binding, making this theory unlikely (Brewster *et al.*, submitted). Further, in the ATP pocket closure model, we see the EXT-hp moving directly around the exit of the side channel, a location suitable for the engagement with DNA from the side channel.

These features all seem to suggest that the side-channel may be utilized for ssDNA passage. If the strand separation occurs at the H2I-hp in the central channel near the internal exit of the side channel, the separated ssDNA would be able to make its way out of the hexamer through the nearby side channel. Thus, the unwinding models for a single hexamer proposed in Figures 2E and 2G, or for a double hexamer in Figures 2F and 2H, could all be likely modes of action for unwinding in *in vitro* experimental conditions and *in vivo* replication.

The side channel paradox

In most of the unwinding models described in Figure 2, the side channels between pairs of subunits are proposed as a possible route of extruding single stranded DNA during unwinding. These side channels may simply be a byproduct of the structure during hexamer assembly, and could play no functional roles. However, as discussed above, the positioning of the important hairpins in the side channels, together with mutational evidence showing the relevance of side channel residues for unwinding in MCM (McGeoch *et al.*, 2005; Brewster *et al.*, 2008) and LTag (Wang *et al.*, 2007), gives tantalizing evidence that the side channels may be utilized during DNA unwinding. The paradox: there are six side channels per hexamer (12 in a double hexamer), but only one or two of the six side channels will be used for ssDNA exit in these unwinding models.

A recent study on MCM using mutant doping experiments relevant to this discussion is by Moreau *et al.*, (2007). In these tests, wild-type and ATP hydrolysis mutants are mixed in varying proportions and activity is measured. From these assays, it can be determined if the six binding sites randomly hydrolyze ATP independent of each other (probabilistic mechanism) or if there is a sequential mechanism, where one hydrolysis event enables or stimulates the adjacent subunit's ATP hydrolysis. In a probabilistic model, activity falls off linearly as the %mutant increases; in a sequential model, one mutated subunit will poison the entire hexamer and activity will fall off exponentially. The data show a semi-sequential model in this study for ssoMCM (Moreau *et al.*, 2007). Specifically, up to three mutants can be tolerated, as long as the remaining three WT subunits are sequential. This implies that only half of the hexamer is needed to unwind DNA, which in turn means that only one or two side channels are necessary. Also, it may imply that only two to three H2I hairpins are required to split DNA in a plowshare model.

If only a few ATP sites are necessary and only one side channel is needed, the rest of the subunits may have no evolutionary pressure in terms of helicase function and can evolve to specialize. This point may bear some relevance to what we see in eukaryotic MCMs with six different subunits (MCM2-7): dimers of 3/7, 7/4 and 4/6 have ATPase activity while the others do not (Davey *et al.*, 2003; Bochman *et al.*, 2008). Further, mutations in Walker B or arginine finger in the 7/4 and 4/6 dimers affect helicase activity while the same mutations in the other dimers have a smaller effect (see Bochman and Schwacha, 2009). Finally, the MCM 2/5 interface has been recently theorized to form a "gate" which both regulates helicase activity and allows for loading onto dsDNA, thus not directly participating in active unwinding (Bochman and Schwacha, 2007; 2008). The 2/5 interface is likely opposite the 7/4 interface (Davey *et al.*, 2003; Yu *et al.*, 2004), where ATPase and helicase activity seems to be present.

Thus, one of these MCM dimers could be specialized to serve as a side channel for ssDNA extrusion, such as the 7/4 side channel for example, or perhaps at the 2/5 gate, with ATP hydrolysis occurring opposite the side channel. Further, evolutionarily specialized proteins could also allow consistent docking of accessory proteins, such as kinase or polymerase, to a single subunit, allowing a specific arrangement of accessory factors with respect to the side channel orientation, an advantage over the symmetric (or non-differentiated) archaeal MCMs.

Conclusion

The wealth of new data regarding MCM structures and functions has significantly aided the understanding of how MCM works in DNA unwinding and replication. Here, we presented recent progress and insights into the structure and functional relationship of the MCM complex. Many of the detailed mechanisms remain to be resolved by future studies, and clearly more data are needed for a better understanding of the unwinding by these replicative helicases in a cellular setting. We hope

the discussion here can serve as a basis for future studies of MCM functions in DNA unwinding and replication.

Acknowledgements

We thank Lauren Holden for her assistance in editing the manuscript, and Drs. D. Gai and B. Greenleaf for insightful discussions.

Declaration of interest

This work is supported in part by NIH grant R01GM080338 to XC. The authors report no conflicts of interest. The authors alone are responsible for the content and writing of the paper.

References

Alexandrov AI, Botchan MR and Cozzarelli NR. 2002. Characterization of simian virus 40 T-antigen double hexamers bound to a replication fork. The active form of the helicase. J Biol Chem 277:44886–44897.

Anachkova B, Djeliova V and Russev G. 2005. Nuclear matrix support of DNA replication. J Cell Biochem 96:951–961.

Bae B, Chen YH, Costa A, Onesti S, Brunzelle JS, Lin Y, Cann IK and Nair SK. 2009. Insights into the architecture of the replicative helicase from the structure of an archaeal MCM homolog. Structure 17:211–222.

Barry ER, Mcgeoch AT, Kelman Z and Bell SD. 2007. Archaeal MCM has separable processivity, substrate choice and helicase domains. Nucleic Acids Res 35:988–998.

Barry ER, Lovett JE, Costa A, Lea SM and Bell SD. 2009. Intersubunit allosteric communication mediated by a conserved loop in the MCM helicase. Proc Natl Acad Sci USA 106:1051–1056.

Bell SP and Dutta A. 2002. DNA replication in eukaryotic cells. Annu Rev Biochem 71:333–374.

Bochman ML and Schwacha A. 2007. Differences in the single-stranded DNA binding activities of MCM2-7 and MCM467: MCM2 and MCM5 define a slow ATP-dependent step. J Biol Chem 282:33795–33804.

Bochman ML and Schwacha A. 2008. The Mcm2-7 complex has in vitro helicase activity. Mol Cell 31:287–293.

Bochman ML and Schwacha A. 2009. The mcm complex: unwinding the mechanism of a replicative helicase. Microbiol Mol Biol Rev 73:652–683.

Bochman ML, Bell SP and Schwacha A. 2008. Subunit organization of Mcm2-7 and the unequal role of active sites in ATP hydrolysis and viability. Mol Cell Biol 28:5865–5873.

Brewster AS, Wang G, Yu X, Greenleaf WB, Carazo JM, Tjajadia M, Klein MG and Chen XS. 2008. Crystal structure of a near-full-length archaeal MCM: functional insights for an AAA+ hexameric helicase. Proc Natl Acad Sci USA 105:20191–20196.

Brewster AS, Slaymaker IM, Afif SA, and Chen XS. 2010. Mutational analysis of an archaeal MCM exterior hairpin reveals critical residues for helicase activity and DNA binding. Submitted.

Bullock PA. 1997. The initiation of simian virus 40 DNA replication in vitro. Crit Rev Biochem Mol Biol 32:503–568.

Carpentieri F, De Felice M, De Falco M, Rossi M and Pisani FM. 2002. Physical and functional interaction between the mini-chromosome maintenance-like DNA helicase and the single-stranded DNA binding protein from the crenarchaeon Sulfolobus solfataricus. J Biol Chem 277:12118–12127.

Chong JP, Hayashi MK, Simon MN, Xu RM and Stillman B. 2000. A double-hexamer archaeal minichromosome maintenance protein is an ATP-dependent DNA helicase. Proc Natl Acad Sci USA 97:1530–1535.

Cook PR. 1999. The organization of replication and transcription. Science 284:1790–1795.

Costa A, Pape T, Van Heel M, Brick P, Patwardhan A and Onesti S. 2006a. Structural basis of the Methanothermobacter thermautotrophicus MCM helicase activity. Nucleic Acids Res 34:5829–5838.

Costa A, Pape T, Van Heel M, Brick P, Patwardhan A and Onesti S. 2006b. Structural studies of the archaeal MCM complex in different functional states. J Struct Biol 156:210–219.

Davey MJ, Indiani C and O'Donnell M. 2003. Reconstitution of the Mcm2-7p heterohexamer, subunit arrangement, and ATP site architecture. J Biol Chem 278:4491–4499.

Donmez I and Patel SS. 2006. Mechanisms of a ring shaped helicase. Nucleic Acids Res 34:4216–4224.

Enemark EJ and Joshua-Tor L. 2006. Mechanism of DNA translocation in a replicative hexameric helicase. Nature 442:270–275.

Enemark EJ and Joshua-Tor L. 2008. On helicases and other motor proteins. Curr Opin Struct Biol 18:243–257.

Fanning E and Zhao K. 2009. SV40 DNA replication: from the A gene to a nanomachine. Virology 384:352–359.

Fletcher RJ, Bishop BE, Leon RP, Sclafani RA, Ogata CM and Chen XS. 2003. The structure and function of MCM from archaeal *M. Thermoautotrophicum*. Nat Struct Biol 10:160–167.

Fletcher RJ, Shen J, Gãmez-Llorente Y, Martã-N CS, Carazo JM and Chen XS. 2005. Double hexamer disruption and biochemical activities of Methanobacterium thermoautotrophicum MCM. J Biol Chem 280:42405–42410.

Forsburg SL. 2004. Eukaryotic MCM proteins: beyond replication initiation. Microbiol Mol Biol Rev 68:109–131.

Forsburg SL. 2008. The MCM helicase: linking checkpoints to the replication fork. Biochem Soc Trans 36:114–119.

Gai D, Li D, Finkielstein CV, Ott RD, Taneja P, Fanning E and Chen XS. 2004a. Insights into the oligomeric states, conformational changes, and helicase activities of SV40 large tumor antigen. J Biol Chem 279:38952–38959.

Gai D, Zhao R, Li D, Finkielstein CV and Chen XS. 2004b. Mechanisms of conformational change for a replicative hexameric helicase of SV40 large tumor antigen. Cell 119:47–60.

Gómez-Llorente Y, Fletcher RJ, Chen XS, Carazo JM and Martin CS. 2005. Polymorphism and double hexamer structure in the archaeal minichromosome maintenance (MCM) helicase from Methanobacterium thermoautotrophicum. J Biol Chem 280:40909–40915.

Greenleaf WB, Shen J, Gai D and Chen XS. 2008. Systematic study of the functions for the residues around the nucleotide pocket in simian virus 40 AAA+ hexameric helicase. J Virol 82:6017–6023.

Ishimi Y. 1997. A DNA helicase activity is associated with an MCM4, -6, and -7 protein complex. J Biol Chem 272:24508–24513.

Iyer LM, Leipe DD, Koonin EV and Aravind L. 2004. Evolutionary history and higher order classification of AAA+ ATPases. J Struct Biol 146:11–31.

Jenkinson ER and Chong JPJ. 2006. Minichromosome maintenance helicase activity is controlled by N- and C-terminal motifs and requires the ATPase domain helix-2 insert. Proc Natl Acad Sci USA 103:7613–7618.

Kaplan DL, Davey MJ and O'Donnell M. 2003. Mcm4,6,7 uses a "pump in ring" mechanism to unwind DNA by steric exclusion and actively translocate along a duplex. J Biol Chem 278:49171–49182.

Kelman Z and White MF. 2005. Archaeal DNA replication and repair. Curr Opin Microbiol 8:669–676.

Kelman Z, Lee JK and Hurwitz J. 1999. The single minichromosome maintenance protein of Methanobacterium thermoautotrophicum DeltaH contains DNA helicase activity. Proc Natl Acad Sci USA 96:14783–14788.

Laskey RA and Madine MA. 2003. A rotary pumping model for helicase function of MCM proteins at a distance from replication forks. EMBO Rep 4:26–30.

Lau E, Tsuji T, Guo L, Lu SH and Jiang W. 2007. The role of pre-replicative complex (pre-RC) components in oncogenesis. FASEB J 21:3786–3794.

Lee JK and Hurwitz J. 2001. Processive DNA helicase activity of the minichromosome maintenance proteins 4, 6, and 7 complex requires forked DNA structures. Proc Natl Acad Sci USA 98:54–59.

Leon RP, Tecklenburg M and Sclafani RA. 2008. Functional conservation of beta-hairpin DNA binding domains in the Mcm protein of Methanobacterium thermoautotrophicum and the Mcm5 protein of *Saccharomyces cerevisiae*. Genetics 179:1757–1768.

Li D, Zhao R, Lilyestrom W, Gai D, Zhang R, Decaprio JA, Fanning E, Jochimiak A, Szakonyi G and Chen XS. 2003. Structure of the replicative helicase of the oncoprotein SV40 large tumour antigen. Nature 423:512–518.

Liu W, Pucci B, Rossi M, Pisani FM and Ladenstein R. 2008. Structural analysis of the Sulfolobus solfataricus MCM protein N-terminal domain. Nucleic Acids Res 36:3235–3243.

Mastrangelo IA, Hough PV, Wall JS, Dodson M, Dean FB and Hurwitz J. 1989. ATP-dependent assembly of double hexamers of SV40 T antigen at the viral origin of DNA replication. Nature 338:658–662.

McGeoch AT, Trakselis MA, Laskey RA and Bell SD. 2005. Organization of the archaeal MCM complex on DNA and implications for the helicase mechanism. Nat Struct Mol Biol 12:756–762.

Moreau MJ, Mcgeoch AT, Lowe AR, Itzhaki LS and Bell SD. 2007. ATPase site architecture and helicase mechanism of an archaeal MCM. Mol Cell 28:304–314.

Morris PD, Byrd AK, Tackett AJ, Cameron CE, Tanega P, Ott R, Fanning E and Raney KD. 2002. Hepatitis C virus NS3 and simian virus 40 T antigen helicases displace streptavidin from 5′-biotinylated oligonucleotides but not from 3′-biotinylated oligonucleotides: evidence for directional bias in translocation on single-stranded DNA. Biochemistry 41:2372–2378.

Moyer SE, Lewis PW and Botchan MR. 2006. Isolation of the Cdc45/Mcm2-7/GINS (CMG) complex, a candidate for the eukaryotic DNA replication fork helicase. Proc Natl Acad Sci USA 103:10236–10241.

Pape T, Meka H, Chen S, Vicentini G, Van Heel M and Onesti S. 2003. Hexameric ring structure of the full-length archaeal MCM protein complex. EMBO Rep 4:1079–1083.

Patel SS and Picha KM. 2000. Structure and function of hexameric helicases. Annu Rev Biochem 69:651–697.

Pucci B, De Felice M, Rossi M, Onesti S and Pisani FM. 2004. Amino acids of the Sulfolobus solfataricus mini-chromosome maintenance-like DNA helicase involved in DNA binding/remodeling. J Biol Chem 279:49222–49228.

Pucci B, De Felice M, Rocco M, Esposito F, De Falco M, Esposito L, Rossi M and Pisani FM. 2007. Modular organization of the Sulfolobus solfataricus mini-chromosome maintenance protein. J Biol Chem 282:12574–12582.

Remus D, Beuron F, Tolun G, Griffith JD, Morris EP and Diffley JF. 2009. Concerted loading of Mcm2-7 double hexamers around DNA during DNA replication origin licensing. Cell 139:719–730.

Rothenberg E, Trakselis MA, Bell SD and Ha T. 2007. MCM forked substrate specificity involves dynamic interaction with the 5′-tail. J Biol Chem 282:34229–34234.

Sakakibara N, Kasiviswanathan R, Melamud E, Han M, Schwarz FP and Kelman Z. 2008. Coupling of DNA binding and helicase activity is mediated by a conserved loop in the MCM protein. Nucleic Acids Res 36:1309–1320.

Sakakibara N, Kelman LM and Kelman Z. 2009. Unwinding the structure and function of the archaeal MCM helicase. Mol Microbiol 72:286–296.

Sclafani RA, Fletcher RJ and Chen XS. 2004. Two heads are better than one: regulation of DNA replication by hexameric helicases. Genes Dev 18:2039–2045.

Shin JH, Heo GY and Kelman Z. 2009. The *Methanothermobacter thermautotrophicus* MCM helicase is active as a hexameric ring. J Biol Chem 284:540–546.

Simmons DT. 2000. SV40 large T antigen functions in DNA replication and transformation. Adv Virus Res 55:75–134.

Singleton MR, Dillingham MS, Gaudier M, Kowalczykowski SC and Wigley DB. 2004. Crystal structure of RecBCD enzyme reveals a machine for processing DNA breaks. Nature 432:187–193.

Smelkova NV and Borowiec JA. 1997. Dimerization of simian virus 40 T-antigen hexamers activates T-antigen DNA helicase activity. J Virol 71:8766–8773.

Smelkova NV and Borowiec JA. 1998. Synthetic DNA replication bubbles bound and unwound with twofold symmetry by a simian virus 40 T-antigen double hexamer. J Virol 72:8676–8681.

Takahashi TS, Wigley DB and Walter JC. 2005. Pumps, paradoxes and ploughshares: mechanism of the MCM2-7 DNA helicase. Trends Biochem Sci 30:437–444.

Tye BK and Sawyer S. 2000. The hexameric eukaryotic MCM helicase: building symmetry from nonidentical parts. J Biol Chem 275:34833–34836.

Valle M, Chen XS, Donate LE, Fanning E and Carazo JM. 2006. Structural basis for the cooperative assembly of large T antigen on the origin of replication. J Mol Biol 357:1295–1305.

Wang W, Manna D and Simmons DT. 2007. Role of the hydrophilic channels of simian virus 40 T-antigen helicase in DNA replication. J Virol 81:4510–4519.

Wessel R, Schweizer J and Stahl H. 1992. Simian virus 40 T-antigen DNA helicase is a hexamer which forms a binary complex during bidirectional unwinding from the viral origin of DNA replication. J Virol 66:804–815.

You Z, Komamura Y and Ishimi Y. 1999. Biochemical analysis of the intrinsic Mcm4-Mcm6-mcm7 DNA helicase activity. Mol Cell Biol 19:8003–8015.

Yu Z, Feng D and Liang C. 2004. Pairwise interactions of the six human MCM protein subunits. J Mol Biol 340:1197–1206.

Editor: Michael M. Cox